Lett., 12, 729 (1976).
(9) C. D. Cook and G. S. Jauhal, J. Am. Chem. Soc., 90, 1464 (1968); C. J. Nyman, C. E. Wymore, and G. Wilkinson, J. Chem. Soc. A, 561 (1968).
(10) Equations 2 are valid only for diluted mixtures of DMF; data related to pure DMF do not satisfy eq 2 probably because dielectric-constant effects become important.
(11) L. Cattalini, Prog. Inorg. Chem., 13, 263 (1970).
(12) S. L. Regen and G. M. Whitesides, J. Organomet. Chem., 59, 293 (1973).
(13) R. J. Hodges, D. E. Webster, and P. B. Wells, J. Chem. Soc. A, 3230 (1971).
(14) P. Sykes, "The Search for Organic Reaction Pathways", Longman, London, 1972, pp 154–156, and references cited therein.
(15) H. C. Brown, O. H. Wheeler, and K. Ichikawa, Tetrahedron, 1, 214 (1957); H. C. Brown and K. Ichikawa, ibid., 1, 221 (1957).
(16) D. C. Wigfield, Tetrahedron, 35, 449 (1979), and references cited therein.
(17) F. Basolo and R. G. Pearson, "Mechanisms of Inorganic Reactions", Wiley, New York, 1967, pp 403–406.
(18) V. Gutmann, Angew. Chem., Int. Ed. Engl., 9, 843 (1970); Coord. Chem. Rev., 18, 225 (1976).
(19) C. Reichardt, Angew. Chem., Int. Ed. Engl., 18, 98 (1979).
(20) F. W. Fowler, A. R. Katritzky, and R. J. D. Rutherford, J. Chem. Soc. B, 460 (1971).
(21) R. Curci, R. DiPrete, J. O. Edwards, and G. Modena in "Hydrogen-Bonded Solvent Systems", A. K. Kovington and T. Jones, Eds., Taylor and Francis, London, 1968, pp 303–321.
(22) A. G. Cook in "Enamines", A. Gilbert Cook, Ed., Marcel Dekker, New York, 1969, pp 243–245.
(23) P. J. Hayward, D. M. Blake, and C. J. Nyman, Chem. Commun., 987 (1969).
(24) S. Otsuka, A. Nakamura, Y. Tatsumo, and M. Miki, J. Am. Chem. Soc., 94, 3761 (1972); J. P. Collman, M. Kubota, and J. Hosking, Ibid., 89, 4809 (1967).
(25) H. Mimoun, I. Serée de Roch, and L. Sajus, Tetrahedron, 26, 37 (1970).
(26) P. Uguagliati and W. H. Baddley, J. Am. Chem. Soc., 90, 5446 (1968).
(27) R. W. Horn, E. Weissberg, and J. P. Collman, Inorg. Chem., 9, 2367 (1970).
(28) W. B. Beaulieu, G. D. Mercer, and D. M. Roundhill, J. Am. Chem. Soc., 100, 1147 (1978).
(29) J. Valentine, D. Valentine, and J. P. Collman, Inorg. Chem., 10, 219 (1971).
(30) G. O. Ozin, Acc. Chem. Res., 10, 21 (1977); J. K. Burdett, Coord. Chem. Rev., 27, 1 (1978), and references cited therein.
(31) A. Abou-Kais, M. Jarjoui, J. C. Vedrine, and P. C. Gravelle, J. Catal., 47, 399 (1977), and references cited therein.

A Kinetics Study of the Oxidation of Iron(II) by Nitric Acid

Irving R. Epstein,* Kenneth Kustin,* and Linda Joyce Warshaw

Contribution from the Department of Chemistry, Brandeis University, Waltham, Massachusetts 02254. *Received December 26, 1979*

Abstract: The kinetics of the ferrous-nitrate clock reaction have been studied by spectrophotometric and potentiometric techniques at high acid concentration (0.6–2.0 M), ionic strength 2.1 M, and temperature 23 ± 1 °C. Our results as well as those of earlier thermodynamic and kinetics investigations on related systems are used to construct a reaction scheme, the rate equations of which are numerically integrated. The overall reaction $3Fe^{2+} + 4H^+ + NO_3^- \rightleftarrows 3Fe^{3+} + 2H_2O + NO$ can be followed by monitoring the absorbance of the $FeNO^{2+}$ intermediate which is formed, or the potential of the Fe(III)/Fe(II) couple. The observed time, t_{max}, to the absorbance peak at 450 nm varies inversely as $[H^+]_0^2[NO_3^-]_0/[Fe^{2+}]_0^{0.6}$. Added oxynitrogen intermediates accelerate the reaction, while dissolved oxygen is an inhibitor. The reaction scheme consists of seven principal reactions, three of which describe the reduction of nitrate to nitric oxide by ferrous ion, one for the formation of the $FeNO^{2+}$ complex, and three additional reactions which summarize the chemistry of oxynitrogen species in nitric acid solutions. The seven rate equations were integrated numerically, which permitted a computer simulation of the reaction profile. Each calculation required the specification of a set of rate constants and a set of initial concentrations for the seven independent species. All but two of the rate constants were available from the literature; in addition the calculation required the specification of the NO_2 solubility β and a parameter C_0 determining the initial HNO_2 (always present) concentration. The simulations revealed that the major factor which determines t_{max} is the rate of the reaction between nitric oxide and nitrate, which is the rate-determining step (with rate constant k_7) in a sequence of reactions which leads to the oxidation of Fe^{2+} and which is autocatalytic in NO. The model is moderately sensitive to the rate constant for the initial attack of nitric acid on ferrous and to the free parameters C_0 and β, but it is extremely sensitive to the value of k_7. Thus, the data should determine k_7 rather accurately (to a factor of 2), if the basic features of the model are correct. Autocatalytic shutdown occurs when $[HNO_2]$ becomes large enough so that nitrous acid is consumed more rapidly by second-order disproportionation than by reaction with ferrous. Thus, addition of oxynitrogen intermediates to the initial reaction mixture provides a quicker way to build up $[HNO_2]$ to a level where autocatalysis is shut down.

The reaction of ferrous ion with nitric acid has been employed as an analytical tool for well over a century.[1] The formation of a colored ferrous–nitric oxide complex provides the basis for the well-known brown-ring test[2] for the qualitative analysis of nitrates and nitrites. In the absence of a catalyst, the reaction begins quite slowly,[3] rendering it unsuitable for quantitative work, though addition of molybdate greatly accelerates the reaction, making possible accurate determination of nitrate.[4] If the uncatalyzed reaction is allowed to proceed, the rate of disappearance of Fe(II) increases and the color rapidly deepens until the solution suddenly returns to a colorless state. Thus the reaction is a clock reaction, which is apparently autocatalytic.[5]

Surprisingly, the kinetics of the ferrous–nitric acid reaction have not yet been subjected to systematic study. One investigation[5] exists in which the dependence of the reaction time on reactant concentrations was probed, but no explanation was suggested for the data obtained. The related reaction of Fe(II) with nitrous acid has been studied in some detail, primarily by Abel and co-workers,[6] and some data are also available on the kinetics of various reactions involving the oxynitrogen species which are present in nitric acid solution.[7–9] The kinetics of formation and dissociation of the $FeNO^{2+}$ complex have been determined.[10]

In this paper, we present a kinetics study of the Fe(II)–HNO_3 reaction. We have measured the rate of the reaction at various concentrations of the reactant species and of several likely intermediates. These results as well as those of earlier thermodynamic and kinetics investigations on related systems are used to construct a reaction scheme. The rate equations of this scheme are then integrated numerically. This procedure enables us both to compare our model with experiment and to

0002-7863/80/1502-3751$01.00/0

estimate those parameters whose values have not previously been established.

General Considerations

The stoichiometry of the overall reaction between ferrous ion and nitric acid is given by

$$3Fe^{2+} + 4H^+ + NO_3^- \rightleftarrows 3Fe^{3+} + 2H_2O + NO \quad (1)$$

The reaction is essentially irreversible, having a $\Delta G°_{298}$ of -13.1 kcal.[11] The progress of the reaction may be followed either spectrophotometrically or potentiometrically. In the former case, one measures the absorbance of the $FeNO^{2+}$ complex which is formed. Alternatively, a redox electrode can be used to measure the oxidizing power of the solution, determined primarily by the $[Fe^{3+}]/[Fe^{2+}]$ ratio.

The kinetic time course of the reaction is difficult to characterize unambiguously. While one may attempt to define regions of uncatalyzed and autocatalytic growth of the complex, and to measure these rates separately, serious ambiguities arise because these regions have a considerable overlap. The most clear-cut experimental quantities are the time at which the peak absorbance occurs, t_{max}, and the height of this peak, A_{max}. We have therefore focused our attention on the behavior of these values as the initial concentrations are varied.

While relatively little is known about the kinetics of reaction 1, a number of thermodynamic data are available on the reactions of both the ferrous–ferric couple and the various oxynitrogen species likely to play a role in the reaction. These data are presented in the next section.

In addition, the reaction between nitric acid and the product nitric oxide is known to proceed autocatalytically.

$$HNO_3 + 2NO + H_2O = 3HNO_2 \quad (2)$$

Abel and Schmid[7] have proposed the reaction scheme

$$H^+ + NO_3^- + HNO_2 = N_2O_4 + H_2O \quad (3)$$

$$N_2O_4 + 2NO + 2H_2O = 4HNO_2 \quad (4)$$

with reaction 3 constituting the rate-determining step, to account for the observed autocatalysis. This explanation has been supported by later investigators[12,13] working under a variety of conditions.

Finally, Abel, Schmid, and Pollak[6] have studied the reaction of nitrous acid with Fe(II)

$$Fe^{2+} + HNO_2 + H^+ \rightleftarrows Fe^{3+} + NO + H_2O \quad (5)$$

and have shown that the reaction proceeds according to a three-term rate law

$$d[Fe^{3+}]/dt = [Fe^{2+}][HNO_2](k_1 + k_2[H^+] + k_3([HNO_2]/[NO])) \quad (6)$$

Our efforts to construct a mechanism for reaction 1 must take into account all of the above observations as well as our own experimental results.

Thermodynamics

In addition to the reactant and product species contained in eq 1, several other species may play a part in the reaction. These include $FeNO^{2+}$, which forms the basis for the spectrophotometric measurement procedure, and several oxynitrogen species including N_2O_4, NO_2, HNO_2, NO_2^-, and N_2O_3. We shall assume that, at the high acidity employed in this study, nitrogen-containing species with lower oxidation states, such as N_2 and N_2O, play no significant role.

The reduction potentials for a number of reactions involving the above species have been determined, and the values given by Latimer[11] are summarized below:

$$Fe^{3+} + e^- = Fe^{2+} \qquad E_7° = 0.771\ V \quad (7)$$

$$NO_3^- + 3H^+ + 2e^- = HNO_2 + H_2O \qquad E_8° = 0.94\ V \quad (8)$$

$$NO_3^- + 4H^+ + 3e^- = NO + 2H_2O \qquad E_9° = 0.96\ V \quad (9)$$

$$2NO_3^- + 4H^+ + 2e^- = N_2O_4 + 2H_2O \qquad E_{10}° = 0.80\ V \quad (10)$$

$$N_2O_4 + 2H^+ + 2e^- = 2HNO_2 \qquad E_{11}° = 1.07\ V \quad (11)$$

$$N_2O_4 + 4H^+ + 4e^- = 2NO + 2H_2O \qquad E_{12}° = 1.03\ V \quad (12)$$

$$HNO_2 + H^+ + e^- = NO + H_2O \qquad E_{13}° = 1.00\ V \quad (13)$$

Standard states of all species are 1 M aqueous, with the exception of N_2O_4 and NO, for which the standard state is the gas phase. The solubility of NO (g, 1 atm) in water at 25 °C is[14] 1.9×10^{-3} M. Further discussion of the N_2O_4–NO_2 solubility appears below.

Equilibrium constants have been determined for several other reactions of interest. These include[15-18]

$$HNO_2(aq) = H^+(aq) + NO_2^-(aq) \qquad K_{14} = 5.1 \times 10^{-4}\ M \quad (14)$$

$$2NO_2(g) = N_2O_4(g) \qquad K_{15} = 8.8\ atm^{-1} \quad (15)$$

$$N_2O_3(g) = NO(g) + NO_2(g) \qquad K_{16} = 1.52\ atm \quad (16)$$

$$Fe^{2+}(aq) + NO(g) = FeNO^{2+}(aq) \qquad K_{17} = 9.1 \times 10^{-1}\ atm^{-1} \quad (17)$$

All values are at 25 °C. Gray and Yoffee[9a] note that K_{15} has been measured in several nonaqueous solvents and is always greater in solution than in the gas phase. These thermodynamic data will be of considerable assistance in our attempts to establish the kinetics parameters of the reaction.

Proposed Reaction Scheme

Choice of Independent Species. We have mentioned above a number of species which may take part in the reaction. The literature contains references to many other species[9] which may be present in solutions containing nitric acid and/or nitric oxide. In order to render the problem tractable, we have chosen to limit our basic reaction scheme to seven major kinetically independent species. Some of the reactions of our proposed scheme will not be elementary reactions, as they may proceed through intermediates not included in our primary set of reactions. We discuss the identity of some of these possible intermediates in the section to follow.

We assume that reactions 14–16 and, in particular, their counterparts in solution proceed very rapidly compared with the other reactions involved and may be taken to be at equilibrium. This assumption permits us to eliminate NO_2^-, N_2O_4, and N_2O_3 as independent species; their concentrations are determined by those of HNO_2, NO_2, NO, and H^+ and the relevant equilibrium constants. We further assume that dissociation of nitric acid is rapid and essentially total,[11] so that we need consider only NO_3^- and not HNO_3. Finally, the concentration of Fe^{3+} is obtained from the initial concentration of Fe^{2+} and the iron mass balance relation.

The major kinetically independent species with which we shall describe the system are then NO_3^-, H^+, Fe^{2+}, HNO_2, NO_2, NO, and $FeNO^{2+}$.

Principal Reactions. Our reaction scheme consists of seven principal reactions, three of which describe the reduction of nitrate to nitric oxide by ferrous ion, one for the formation of the $FeNO^{2+}$ complex, and three additional reactions which summarize the chemistry of oxynitrogen species in nitric acid solution. All principal reactions (designated P1–P7) are written in terms of aqueous species. Their equilibrium constants may be calculated from the thermodynamic data given in eq 7–17, the solubility of NO, and the solubility of NO_2, which we designate as β ($M\ atm^{-1}$).

The reaction sequence is initiated by the attack of Fe^{2+} on nitrate:

$$Fe^{2+} + NO_3^- + 2H^+ = Fe^{3+} + NO_2 + H_2O \qquad K1 = 1.0\beta\ M^{-2} \quad (P1)$$

The one-electron reductant Fe^{2+} then goes on to reduce nitrogen further to N(II) in steps P2 and P3:

$$Fe^{2+} + NO_2 + H^+ = Fe^{3+} + HNO_2 \qquad K2 = 3.4 \times 10^5/\beta\ M^{-1} \quad (P2)$$

$$Fe^{2+} + HNO_2 + H^+ = Fe^{3+} + NO + H_2O \qquad K3 = 1.4 \times 10^1\ M^{-1} \quad (P3)$$

The complex formation is described by the reaction

$$Fe^{2+} + NO = FeNO^{2+} \qquad K4 = 4.5 \times 10^2\ M^{-1} \quad (P4)$$

In addition, in nitric acid solution we may expect the hydrolysis of NO_2, the disproportionation of nitrous acid, and the reaction between nitric acid and nitric oxide to play major roles:

$$2NO_2 + H_2O = HNO_2 + NO_3^- + H^+ \qquad K5 = 3.2 \times 10^5/\beta^2\ M \quad (P5)$$

$$2HNO_2 = NO + NO_2 + H_2O \qquad K6 = 4.2 \times 10^{-5}\beta \quad (P6)$$

$$NO + NO_3^- + H^+ = NO_2 + HNO_2 \qquad K7 = 7.7 \times 10^{-2}\beta\ M^{-1} \quad (P7)$$

We note that reactions P1 + P2 + P3 give the overall stoichiometry of reaction 1, while reactions P5 + P6 + P7 result in no net reaction.

Kinetics Considerations

Several of our principal reactions have been studied by previous investigators and their rate laws and rate constants established. For the remainder, we present arguments based on our experimental data and the results of computer simulation of the reaction by numerical integration of the rate equations.

Reaction P1. Ferrous ion is a one-electron reductant, and its initial reaction should therefore be to reduce nitrate to N(IV). No kinetics data could be found in the literature for reaction P1, but it is clear from the very slow initial buildup of Fe^{3+} that this step must be quite slow. We postulate that (P1) occurs in two steps, the first of which involves a bimolecular reaction of Fe^{2+} with NO_3^-. This reaction may occur via outer-sphere or inner-sphere electron transfer. One possibility for the former is

$$Fe^{2+} + NO_3^- = Fe^{3+} + NO_3^{2-} \quad \text{(slow)} \quad (18)$$

$$NO_3^{2-} + 2H^+ = H_2O + NO_2 \quad \text{(rapid)} \quad (19)$$

with the rate for step P1 then given by

$$v_1 = k_1[Fe^{2+}][NO_3^-] \quad (20)$$

$$v_{-1} = k_{-1}\frac{[Fe^{3+}][NO_2]}{[H^+]^2} \quad (21)$$

where v_i and v_{-i} are the forward and reverse rates, respectively, for the ith principal reaction. The NO_3^{2-} ion is known to form in pulse radiolysis experiments by the addition of e^-_{aq} to nitrate.[19] Fe^{2+} is a weaker reductant than e^-, however, and an alternative possibility is inner-sphere electron transfer[20] (eq 22 and 23).

Our computer simulations indicate that, as long as k_1 is not too large, the course of the reaction is relatively insensitive to the value employed for k_1. We choose the value $k_1 = 1.5 \times 10^{-4}\ M^{-1}\ s^{-1}$. The equilibrium constant $K1$ then requires that the rate constant k_{-1} be $k_{-1} = 1.5 \times 10^{-4}/\beta\ M\ s^{-1}$.

$$Fe^{2+} + NO_3^- = \left(Fe{-}O{-}N\begin{matrix}O\\O\end{matrix}\right)^+ \quad (22)$$

$$\left(Fe{-}O{-}N\begin{matrix}O\\O\end{matrix}\right)^+ + 2H^+ = Fe^{3+} + H_2O + NO_2 \quad (23)$$

Reaction P2. Abel, Schmid, and Pollak[6] found that the reaction

$$Fe^{2+}(aq) + NO_2(g) \rightarrow Fe^{3+}(aq) + NO_2^-(aq) \quad (24)$$

proceeds with the rate law

$$d[Fe^{3+}]/dt = k_{24}[Fe^{2+}]P_{NO_2}$$

where $k_{24} = 1.3 \times 10^4\ atm^{-1}\ min^{-1}$. If we introduce the rapid equilibrium (14) and the solubility of NO_2, we obtain for the forward rate of (P2)

$$v_2 = k_2[Fe^{2+}][NO_2] \quad (25)$$

with $k_2 = 2.2 \times 10^2/\beta\ M^{-1}\ s^{-1}$. From the equilibrium constant for (P2) we obtain

$$v_{-2} = k_{-2}\frac{[Fe^{3+}][HNO_2]}{[H^+]} \quad (26)$$

with $k_{-2} = 6.6 \times 10^{-4}\ s^{-1}$.

Reaction P3. The reaction between ferrous ion and nitrous acid was found by Abel, Schmid, and Pollak[6] to proceed according to a three-term rate law

$$d[Fe^{3+}]/dt = [Fe^{2+}][HNO_2](k'_{3a} + k'_{3b}[H^+] + k'_{3c}([HNO_2]/P_{NO})) \quad (27)$$

The three rate constants were found to have the values $k'_{3a} = 0.47\ M^{-1}\ min^{-1}$, $k'_{3b} = 13.6\ M^{-2}\ min^{-1}$, and $k'_{3c} = 2.4 \times 10^2\ M^{-2}\ atm\ min^{-1}$. The mechanisms for the three pathways were proposed to be[21]

(a) $Fe^{2+} + HNO_2 = Fe^{3+} + OH^- + NO$ (slow) (28)
$H^+ + OH^- = H_2O$ (rapid) (29)

(b) $HNO_2 + H^+ = H_2NO_2^+$ (rapid) (30)
$H_2NO_2^+ = H_2O + NO^+$ (rapid) (31)
$Fe^{2+} + NO^+ = Fe^{3+} + NO$ (slow) (32)

(c) $2HNO_2 = NO_2 + NO + H_2O$ (rapid) (33)
$Fe^{2+} + NO_2 = NO_2^- + Fe^{3+}$ (slow) (34)
$H^+ + NO_2^- = HNO_2$ (rapid) (35)

We note that reaction 34 is just reaction 24 and reaction 33 is our reaction P6, so that k'_{3c} may be calculated from k_{24} and $K6$.

Converting the times to seconds and using the solubility of NO, we may write eq 27 as

$$v_3 = [Fe^{2+}][HNO_2](k_{3a} + k_{3b}[H^+] + k_{3c}([HNO_2]/[NO])) \quad (36)$$

where $k_{3a} = 7.8 \times 10^{-3}\ M^{-1}\ s^{-1}$, $k_{3b} = 2.3 \times 10^{-1}\ M^{-2}\ s^{-1}$, and $k_{3c} = 7.6 \times 10^{-3}\ M^{-1}\ s^{-1}$. Using the equilibrium constant $K3$ and detailed balance, we also have

$$v_{-3} = [Fe^{3+}](k_{-3a}([NO]/[H^+]) + k_{-3b}[NO] + k_{-3c}([HNO_2]/[H^+])) \quad (37)$$

where $k_{-3a} = 5.6 \times 10^{-4}\ s^{-1}$, $k_{-3b} = 1.6 \times 10^{-2}\ M^{-1}\ s^{-1}$, and $k_{-3c} = 5.4 \times 10^{-4}\ s^{-1}$.

Reaction P4. Kustin, Taub, and Weinstock[10] have measured the rates of $FeNO^{2+}$ formation and decomposition spectrophotometrically using a temperature-jump technique. They obtained

$$v_4 = k_4[Fe^{2+}][NO] \quad (38)$$

$$v_{-4} = k_{-4}[FeNO^{2+}] \quad (39)$$

with $k_4 = 6.2 \times 10^5\ M^{-1}\ s^{-1}$ and $k_{-4} = 1.4 \times 10^3\ s^{-1}$.

Reaction P5. The kinetics of the hydrolysis of N_2O_4 were studied by Abel and co-workers[7,8] as part of their investigation of reaction 2. They measured the rates of both the forward and the reverse reactions in eq 3 in terms of $P_{N_2O_4}$ and the concentrations of the aqueous species. Using the NO_2-N_2O_4 equilibrium constant, we have

$$v_5 = k_5[NO_2]^2 \quad (40)$$

$$v_{-5} = k_{-5}[HNO_2][NO_3^-][H^+] \quad (41)$$

where $k_5 = 8.4 \times 10^3/\beta^2\ M^{-1}\ s^{-1}$ and $k_{-5} = 2.7 \times 10^{-2}\ M^{-2}\ s^{-1}$. An attempt[22] was made to generate NO_2 in situ and determine the rate of hydrolysis directly. The decomposition proved to be complex, and the only certain conclusion drawn was that the hydrolysis was very rapid.

Reaction P6. The disproportionation of HNO_2 is actually the reverse of Abel and Schmid's[7] reaction 4. Those authors were able to conclude only that reaction 4 must be more rapid than reaction 3, in order that reaction 2 be autocatalytic in HNO_2. A rate constant is available, however, from the study of Bunton, Llewellyn, and Stedman[23] on oxygen exchange between nitrous acid and water. Their work gives

$$v_6 = k_6[HNO_2]^2 \quad (42)$$

with $k_6 = 5.8\ M^{-1}\ s^{-1}$, and use of the equilibrium constant for (16) yields

$$v_{-6} = k_{-6}[NO][NO_2] \quad (43)$$

with $k_{-6} = 1.4 \times 10^5/\beta\ M^{-1}\ s^{-1}$.

Reaction P7. Although reaction P7 has been suggested[24] as a significant one in solutions containing oxynitrogen species, we were unable to find any data on its kinetics in the literature. Our computer simulations reveal that the major factor which determines t_{max} is the rate of reaction P7. This observation can be understood by noting that the net reaction (P2) + 2(P3) + (P7) is the overall reaction eq 1, and that, if (P7) is slower than (P2) and (P3), the rate will be proportional to [NO]; i.e., the oxidation of Fe^{2+} will be autocatalytic in NO.

In view of the strong dependence of t_{max} on $[H^+]$, we suggest that (P7) occurs via the mechanism

$$2H^+ + NO_3^- = H_2NO_3^+ \quad \text{(rapid)} \quad (44)$$

$$H_2NO_3^+ + NO = HNO_2 + NO_2 + H^+ \quad \text{(slow)} \quad (45)$$

The postulated intermediate $H_2NO_3^+$ is a reasonable one[25] at the acidities employed here, and reaction 44 should certainly be rapid.

With this mechanism the rate law for (P7) becomes

$$v_7 = k_7[NO_3^-][NO][H^+]^2 \quad (46)$$

$$v_{-7} = k_{-7}[HNO_2][NO_2][H^+] \quad (47)$$

Since the simulated values of t_{max} increase sharply as k_7 is decreased, we can get a good estimate of that value from a comparison of our experimental and calculated values. We take $k_7 = 7.5\ M^{-3}\ s^{-1}$, which implies that $k_{-7} = 9.8 \times 10^1/\beta\ M^{-2}\ s^{-1}$.

Initial Concentrations of Intermediates. In their study of the autocatalytic production of nitrous acid from nitric acid and nitric oxide, eq 2, Schmid and Bähr[12] note that there is always a small amount of HNO_2 present initially in their nitric acid solutions. This observation plays an important role in our reaction scheme, and we assume that some HNO_2 is present initially in our solutions as well. We take the amount of HNO_2 to be proportional to the concentration of nitric acid according to the equation

$$[HNO_2]_0 = C_0[H^+]_0[NO_3^-]_0 \quad (48)$$

where the subscript 0 denotes initial concentrations. We also assume that this HNO_2 present initially has had time to equilibrate with NO and NO_2 according to eq P6. The results of the computer simulations are profoundly affected by the presence of these initial intermediates (v_3 diverges without them; see eq 36), but the kinetic behavior is not particularly sensitive either to the numerical value assigned to C_0 or to the functional form of eq 48.

Integration of Rate Equations. Our set of equations (P1) to (P7) was integrated numerically using Hindmarsh's version[26] of a method due to Gear[27] which is designed to deal with the wide range of time constants occurring in kinetics problems like this one. All calculations were performed in double-precision arithmetic on the Brandeis PDP-10 computer. Each calculation required the specification of a set of rate constants for reactions P1-P7 and a set of initial concentrations for our seven independent species. There were thus four free parameters: the rate constants k_1 and k_7, the constant determining the initial HNO_2 concentration C_0, and the NO_2 solubility β.

NO_2 Solubility. Since several of the rate and equilibrium constants which appear in our scheme were determined for reactions involving gaseous NO_2 (or N_2O_4), the NO_2 solubility β is required in order for us to obtain the corresponding quantities in solution. A search of the literature failed to uncover a value for β, though some experiments have been carried out[28] under conditions quite different from those of interest here. Those results show significant deviations from Henry's law and do not lend themselves to extrapolation to the present conditions. Use of more general methods of calculating gas solubilities[29] also requires more data than are available here.

Abel and Schmid's conclusion[7] that the rate of reaction 4 exceeds that of reaction 3 implies that $k_5 > k_{-6}$ in our reaction scheme. Taking into account the dependence of these quantities on β (eq 40-43) we obtain an upper limit on the solubility, $\beta < 6.0 \times 10^{-2}\ M\ atm^{-1}$. A reasonable lower limit would seem to be the solubility of NO, i.e., $\beta > 1.9 \times 10^{-3}\ M\ atm^{-1}$. We have employed a value of $\beta = 1.9 \times 10^{-2}\ M\ atm^{-1}$ in our numerical simulations, though, as noted in the Discussion, the results obtained are quite insensitive to variations in β between these upper and lower limits.

Activity Coefficient Corrections. All the experiments in this study were performed at an ionic strength $\mu = 2.1$ M. The thermodynamic values employed and the kinetic parameters given above for reactions P2, P3, and P5 were either measured at low ionic strengths ($\mu \lesssim 0.1$ M) or extrapolated to $\mu = 0$. At the ionic strength employed here, activity coefficient corrections can be expected to be significant, at least for those steps in which two or more ions are involved.

For reaction P5, Abel and Schmid[7] report rate constants over a range of ionic strengths between 0 and 2.5 M. Their value for k_5 varies linearly with μ, while their data for k_{-5} correspond roughly to a simple Debye-Hückel limiting law dependence (cf. eq 41).

$$v_{-5} = k_{-5}^0\gamma_\pm^2[HNO_2][NO_3^-][H^+] \quad (49)$$

where

$$\log \gamma_\pm = 0.50 z_1 z_2 \mu^{1/2} \quad (50)$$

and z_1 and z_2 are the charges on the ions, in this case -1 and $+1$.

Corrections of the form of eq 50 are expected to break down at ionic strengths well below the value employed here. Since our aim is a qualitative understanding of the system and since the calculation of activity coefficients at high ionic strengths by more sophisticated techniques is a risky procedure at best, we have nonetheless introduced such corrections in those steps

Table I. Reaction Scheme and Kinetics Parameters Employed in Computer Simulations[a]

no.	reaction and velocity
(P1)	$Fe^{2+} + NO_3^- + 2H^+ = Fe^{3+} NO_2 + H_2O$
	$v_1 = 1.0 \times 10^{-6}\ M^{-1}\ s^{-1}[Fe^{2+}][NO_3^-]$
	$v_{-1} = 2.8 \times 10^{-4}\ M\ s^{-1}[Fe^{3+}][NO_2]/[H^+]^2$
(P2)	$Fe^{2+} + NO_2 + H^+ = Fe^{3+} + HNO_2$
	$v_2 = 1.2 \times 10^4\ M^{-1}\ s^{-1}[Fe^{2+}][NO_2]$
	$v_{-2} = 2.3 \times 10^{-5}\ s^{-1}[Fe^{3+}][HNO_2]/[H^+]$
(P3)	$Fe^{2+} + HNO_2 + H^+ = Fe^{3+} + NO + H_2O$
	$v_3 = (7.8 \times 10^{-3}\ M^{-1}\ s^{-1} + 3.4 \times 10^1\ M^{-2}\ s^{-1}[H^+] + 7.6 \times 10^{-3}\ M^{-1}\ s^{-1}[HNO_2]/[NO]) \times [Fe^{2+}][HNO_2]$
	$v_{-3} = (1.6 \times 10^{-2}\ s^{-1}[NO]/[H^+] + 1.6 \times 10^{-2}\ M^{-1}\ s^{-1}[NO] + 1.5 \times 10^{-2}\ s^{-1}[HNO_2]/[H^+])[Fe^{3+}]$
(P4)	$Fe^{2+} + NO = FeNO^{2+}$
	$v_4 = 6.2 \times 10^5\ M^{-1}\ s^{-1}[Fe^{2+}][NO]$
	$v_{-4} = 1.4 \times 10^3\ s^{-1}[FeNO^{2+}]$
(P5)	$2NO_2 + H_2O = HNO_2 + NO_3^- + H^+$
	$v_5 = 2.3 \times 10^7\ M^{-1}\ s^{-1}[NO_2]^2$
	$v_{-5} = 9.6 \times 10^{-4}\ M^{-2}\ s^{-1}[HNO_2][NO_3^-][H^+]$
(P6)	$2HNO_2 = NO + NO_2 + H_2O$
	$v_6 = 5.8\ M^{-1}\ s^{-1}[HNO_2]^2$
	$v_{-6} = 7.4 \times 10^6\ M^{-1}\ s^{-1}[NO][NO_2]$
(P7)	$NO + NO_3^- + H^+ = NO_2 + HNO_2$
	$v_7 = 5.0 \times 10^{-2}\ M^{-3}\ s^{-1}[NO_3^-][NO][H^+]^2$
	$v_{-7} = 9.7 \times 10^2\ M^{-2}\ s^{-1}[HNO_2][NO_2][H^+]$

[a] $\beta = 1.9 \times 10^{-2}$ M atm^{-1}, $\mu = 2.1$ M, $[HNO_2]_0 = 2.0 \times 10^{-6}$ $M^{-1}[H^+]_0[NO_3^-]_0$.

in which two or more ions react, namely, (P1), (P−1), (P−2), (P3b), (P−3a), (P−3c), (P−5), and (P7). We recognize that the rate constants thus obtained are probably accurate to no better than an order of magnitude. The values employed in the simulations are given in Table I.

Results

A series of experiments were performed in which the reaction was followed spectrophotometrically at 450 nm, where the absorbance of species other than the $FeNO^{2+}$ complex is negligible. A typical trace is shown in Figure 1 along with the computer simulation for the initial concentrations employed. We see that, although the absorbance at the peak is overestimated somewhat, the model qualitatively reproduces the slow initial rise in absorbance followed by a rapid autocatalytic buildup of $FeNO^{2+}$ and then a sharp dropoff. Several runs were also made in which the reaction was monitored potentiometrically. A typical case is plotted in Figure 2. Since we are now measuring the ratio of oxidized to reduced iron rather than the concentration of complex, no falloff occurs after the maximum; the potential simply remains constant.

In Figure 3 we show how the observed time t_{max} to the absorbance peak varies with the initial concentrations of H^+, NO_3^-, and Fe^{2+}. In all cases the ionic strength has been adjusted to 2.1 M by addition of $NaClO_4$. The slopes of the experimental log-log plots are $d \ln 1/t_{max}/d \ln[X]_0 = 2.01 \pm 0.08$, 0.99 ± 0.05, and -0.58 ± 0.04 for $X = H^+$, NO_3^-, and Fe^{2+}, respectively, while the corresponding slopes from the computer simulation are 1.89, 1.08, and −0.78. The variation in A_{max} is reproduced less well by our model. Although the general trend that A_{max} decreases with $[H^+]_0$ and $[NO_3^-]_0$ and increases with $[Fe^{2+}]_0$ is seen, the experimental peak absorbances vary considerably more sharply with initial concentrations than do the calculated values.

In addition to varying the reactant concentrations, we also monitored the reaction in the presence of added oxynitrogen species. In Figure 4 we plot our observed and calculated values of A_{max} and t_{max} as a function of the initial concentration of $NaNO_2$ added to the reaction mixture. Again, the quantitative

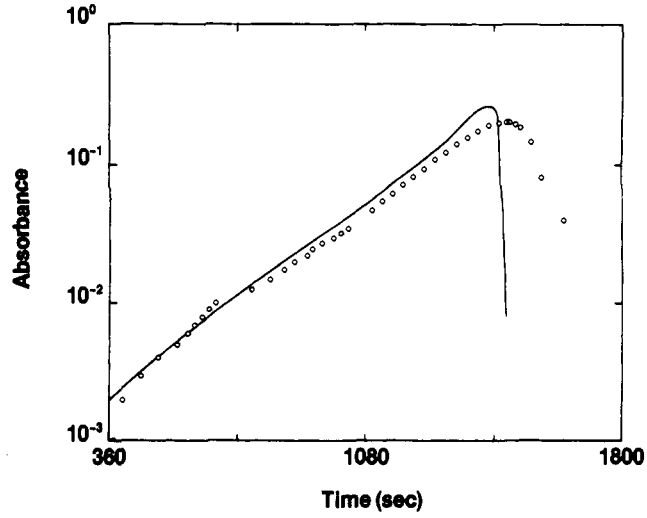

Figure 1. Absorbance at 450 nm vs. time for a solution containing initial concentrations of $[Fe^{2+}]_0 = 0.025$ M, $[NO_3^-]_0 = 1.0$ M, $[H^+]_0 = 1.0$ M, and ionic strength $\mu = 2.1$ M. Circles are experimental points; solid line is computer simulation. The absorbance falloff in the simulation is probably more realistic than in the experiment because of the finite pen response time.

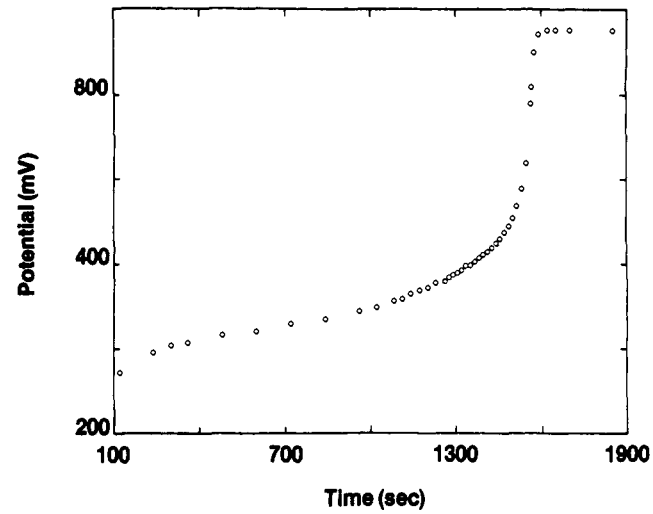

Figure 2. Measured potential (uncalibrated) vs. time for a redox electrode in a solution with $[Fe^{2+}]_0 = 0.025$ M, $[NO_3^-]_0 = 1.0$ M, $[H^+]_0 = 1.0$ M, $\mu = 2.1$ M.

values of A_{max} are significantly in error, though the calculation does reproduce the insensitivity of A_{max} to $[NO_2^-]_0$. We see that the observed decrease of t_{max} with $[NO_2^-]$ is in good agreement with the simulated values. The ineffectiveness of nitrite additions below $\sim 2 \times 10^{-6}$ M in accelerating the reaction suggests that C_0 in eq 48 has a magnitude comparable to this value.

A similar set of experiments was performed to assess the effects of initial addition of NO and NO_2. The NO additions were accomplished by adding saturated solutions of the gas to the other reactants. The NO(aq) concentration was estimated from the solubility. Added NO also accelerates the reaction and for the same value of $[NO]_0$ and $[NO_2^-]_0$ the acceleration produced by the NO addition appears to be somewhat greater, although this may be an artifact of supersaturation. Bubbling nitrogen dioxide through the solution initially gives qualitatively similar effects, but no quantitative data were obtained because of the uncertainty as to the value of the NO_2 solubility. Computer simulation gives results nearly identical with those shown in Figure 4 for both NO and NO_2 addition.

In their study of reaction 2, Schmid and Bähr[12] found that

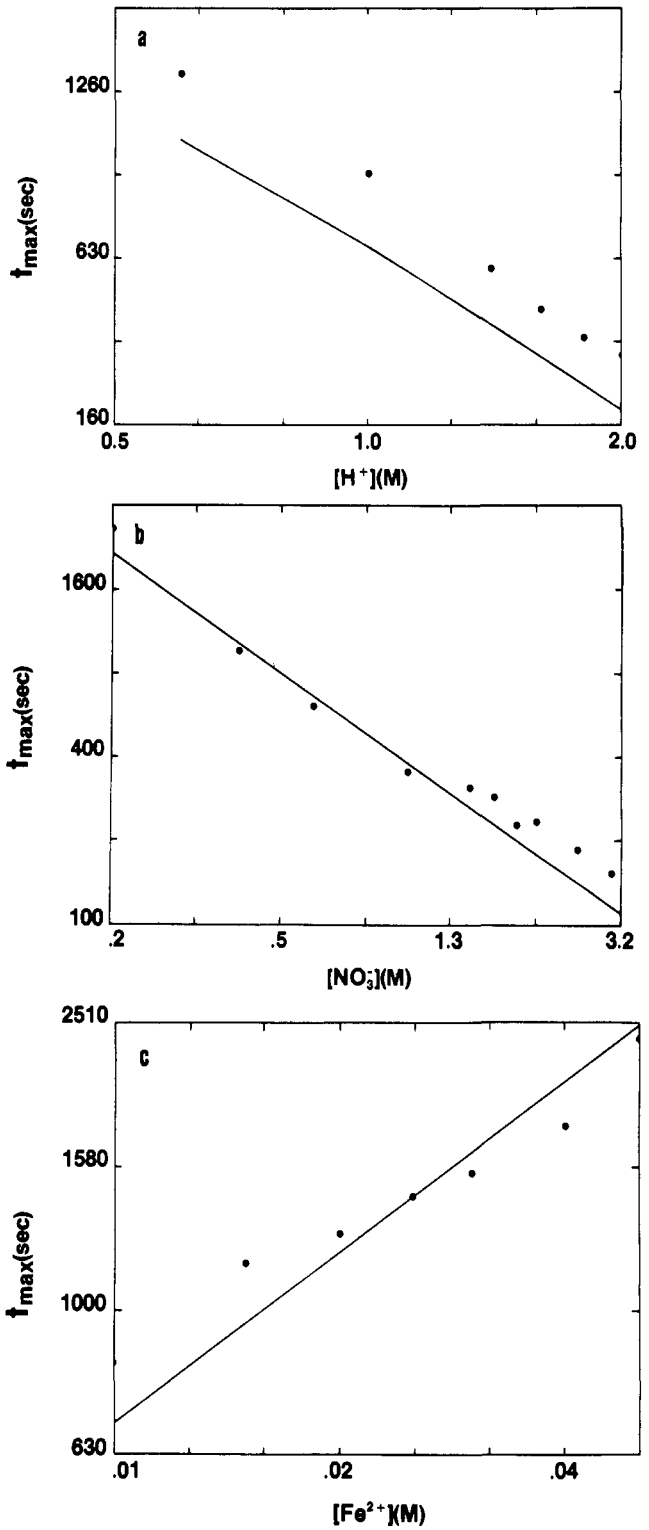

Figure 3. Log-log plots of t_{max} vs. (a) $[H^+]_0$, (b) $[NO_3^-]_0$ (c) $[Fe^{2+}]_0$. Circles are experimental points; solid lines are computer simulations. In all cases μ = 2.1 M. In (a) $[Fe^{2+}]_0$ = 0.025 M, $[NO_3^-]_0$ = 2.0 M; in (b) $[Fe^{2+}]_0$ = 0.025 M, $[H^+]_0$ = 2.0 M; in (c) $[NO_3^-]_0 = [H^+]_0$ = 1.0 M.

additions of small but unspecified quantities of sodium azide removed the HNO_2 initially present in their nitric acid solutions and permitted study of the initial reaction in the absence of the autocatalytic product. We found that addition of $>1.4 \times 10^{-3}$ M azide to our initial reaction mixture containing 1 M H^+ and NO_3^- and 0.025 M Fe^{2+} totally inhibited the reaction, while an initial $[N_3^-]$ of 2.2×10^{-6} M led to an 11% increase in reaction time. These results are again suggestive of a value of C_0 of about 10^{-6} M^{-1}.

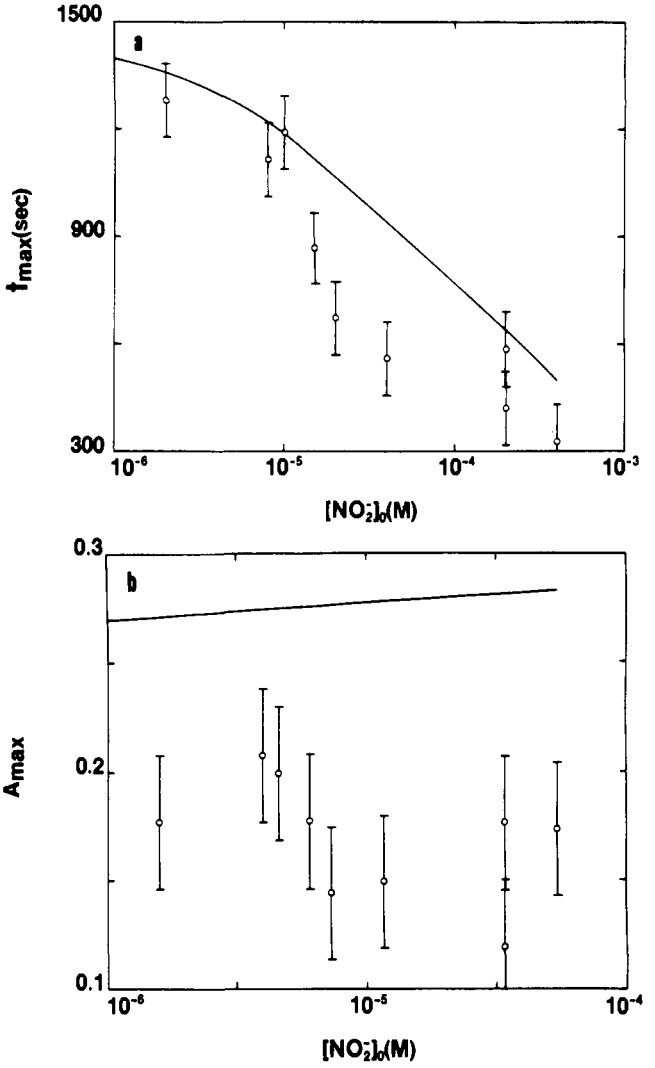

Figure 4. (a) t_{max} and (b) A_{max} vs. added $[NO_2^-]_0$ for solutions with $[Fe^{2+}]$ = 0.025 M, $[NO_3^-]_0 = [H^+]_0$ = 1.0 M. Circles are experimental points; solid lines are computer simulations.

The presence of oxygen appears to exert some influence on the reaction. If the solutions are ultrasonicated and saturated with argon prior to reaction, t_{max} is reduced slightly from its value in the absence of this procedure. Bubbling oxygen through the solution for the entire course of the reaction lengthens t_{max} significantly (from 22 to 31 min for a typical reaction) and inhibits complex formation to the point that the peak is only just observable. Presumably these observations result from the rapid oxidation of NO to NO_2 which inhibits both reaction P4 and P7.

Discussion

With the availability of numerical methods for treating large sets of stiff coupled differential equations,[27] the approach employed here of combining experimental studies with integration of a set of model equations[31] has proved increasingly fruitful in elucidating the kinetics of complex systems for which one or more individual rate constants may be inaccessible to direct measurement. Recent work has successfully applied this technique to the oscillatory Belousov–Zhabotinskii reaction[32] and to the oxidation of ferrous ion by iodate in acid media.[33] However, as Sullivan and Thompson[34] point out, one must be extremely cautious in drawing quantitative inferences about rate constants from the results of numerical simulations.

In order to assess the sensitivity of our results to the free parameters k_1, k_7, C_0, and β, we have varied each of these

within rather broad limits. Increase in k_1 by a factor of 100 cuts t_{max} by a factor of about 3, produces an initial rate of increase of $[FeNO^{2+}]$ considerably greater than observed, and weakens the dependence of t_{max} on $[H^+]_0$ while increasing the variation of t_{max} with $[NO_3^-]_0$. A decrease in k_1 by a factor of 100 produces a 25% increase in t_{max}, which can be compensated by a small increase in k_7 without changing the overall kinetic behavior.

The model is extremely sensitive to the value of k_7. Doubling or halving the value of k_7 produces a 1.8-fold decrease or increase, respectively in t_{max} and about a 10% decrease or increase in the maximum absorbance. Tenfold variation in k_7 changes t_{max} by a factor of 7–8. Thus, if the basic features of our model are correct, the data should determine k_7 rather accurately, certainly to within a factor of 2.

The other free parameters C_0 and β exert considerably less influence on the kinetics of our model. Decreasing C_0 by a factor of 100 produces an increase in t_{max} of less than 10%. Although an increase in C_0 significantly accelerates the appearance of the peak, values much larger than that used here appear to be ruled out by our initial NO and azide addition experiments. Variation of the NO_2 solubility by a factor of 100 in either direction, well outside the limits suggested earlier, had almost no effect on the kinetics. Our calculated values of $[NO_2]$ in the absence of added initial nitrogen dioxide never exceeded 10^{-6} M, a value far below the assumed solubility.

Some of the rate and equilibrium constants employed in this study have also been measured by pulse radiolysis techniques[35,36] directly in terms of aqueous nitrogen oxide concentrations in place of the gas-pressure determinations of the earlier workers. As Stedman,[37] who has recently reviewed this work, points out, however, pulse radiolytic measurements are not without their pitfalls, and significant discrepancies exist between values given for the same quantities by different workers. In all cases, the pulse radiolytic rate constants differ from those used in this study by no more than a factor of 2.8, and computer simulations carried out with the pulse radiolytic values give results essentially indistinguishable from those reported above. Comparison of the pulse radiolytic equilibrium and rate constants with the earlier work also enables us to narrow the possible limits on the NO_2 solubility to 1.1×10^{-2} M atm$^{-1} \leq \beta \leq 2.0 \times 10^{-2}$ M atm^{-1}.

From our experimental data and the results of our computer simulations we can now pinpoint the origins of the dependence of the reaction time on the initial reactant concentrations. Reaction P4 is sufficiently rapid with respect to our other principal reactions that (P4) is essentially always at equilibrium. The $FeNO^{2+}$ complex therefore serves simply as an indicator of the concentrations of Fe^{2+} and NO. In the early stages of the reaction, $[Fe^{2+}]$ drops steadily as it is consumed in reactions P1–P3. These reactions also produce a gradual increase in [NO], $[HNO_2]$, and $[NO_2]$. The rate of buildup of the oxynitrogen species begins to accelerate as a result of the autocatalytic sequence, (P2) + 2(P3) + (P7), whose net rate is determined by that of reaction P7. Initial concentrations of NO_3^- and of H^+ greatly exceed that of Fe^{2+} in our experiments; the concentrations of nitrate and of hydrogen ions thus remain nearly constant, and the rate law eq 46 for reaction P7 accounts for the major part of the dependence of the reaction time on the initial nitrate and proton concentrations.

The fractional rate of increase of [NO] during the autocatalytic period is considerably greater than the fractional rate of decrease of $[Fe^{2+}]$, and the $FeNO^{2+}$ absorbance therefore continues to grow until the autocatalytic sequence is interrupted. This shutdown occurs when $[HNO_2]$ becomes large enough so that reaction P6 consumes nitrous acid more rapidly than reaction P3. The nitrous acid disproportionation reaction (P6) thus plays much the same role in our scheme as does the second-order disproportionation of bromous acid in providing a means of controlling the autocatalytic sequence in the Field–Körös–Noyes mechanism[38] for the Belousov–Zhabotinskii reaction. If we view the duration of the reaction as the time required for reaction P6 to "catch up" with reaction P3, it becomes clear why t_{max} should increase with $[Fe^{2+}]_0$, even though the individual reactions of the scheme are all speeded up or unaffected. This point of view also accounts both for the fact that the absorbance at the maximum is more sensitive to $[Fe^{2+}]_0$ than to either of the other initial concentrations and for the positive correlation between the observed values of t_{max} and A_{max}.

Addition of HNO_2, NO_2, or NO to the initial reaction mixture is now seen to provide a quicker way to build up $[HNO_2]$ to a level where the autocatalysis is shut down. This interpretation would suggest, and our experimental data confirm, that the maximum absorbance should be relatively insensitive to the initial concentrations of these species, since the $[Fe^{2+}]$ and [NO] values at t_{max} will be primarily determined by reactions P1–P3.

The concentration profiles of our seven principal species reveal that, as expected, $[Fe^{2+}]$, $[NO_3^-]$, and $[H^+]$ decrease monotonically to their final values, with the rate of consumption being greatest in the neighborhood of t_{max}. After an initial adjustment when the Fe^{2+} is added, $[NO_2]$, $[HNO_2]$, and [NO] all rise at an increasing rate until the peak is reached; $[NO_2]$ and $[HNO_2]$ then continue rising a bit more to their steady-state levels, while NO decreases from its peak value as a result of the reverse reactions of (P3) and (P6) and the forward reaction of (P7).

On the whole, the proposed model seems to explain the shapes of the absorbance and potential vs. time curves and the dependence of t_{max} on the initial reactant and intermediate concentrations quite nicely. While the simulated absorbances are somewhat less sensitive to the reactant concentrations than are the experimental observations, this discrepancy could easily result from inaccuracies in one or more of our free parameters or in our estimates of the activity coefficients at the high ionic strengths employed in this study. In view of the difficulties associated with determining and/or extrapolating most of these parameters, we make no claims of quantitative accuracy for any individual values, though we do feel that the present study provides a qualitative understanding of this interesting and important reaction.

Experimental Section

Materials. High-purity $FeSO_4$, HNO_3, $HClO_4$, $NaClO_4$, NO, NO_2, $NaNO_2$, and NaN_3 were available commercially and were used as received from the manufacturers, with the exception of the sodium azide, which was first recrystallized. Solutions were ultrasonicated before use. Ferrous solutions through which atomic hydrogen was bubbled prior to use gave no different results from solutions not treated in this manner, and all subsequent studies omitted this step. Saturation with argon was found to have no effect and was omitted in subsequent experiments.

Spectrophotometric Analysis. All measurements were made on a Beckman Model 25 spectrophotometer thermostated at 23 ± 1 °C. Solutions were mixed externally and then added to the cell which was placed in the spectrophotometer. This procedure required about 1 min. To determine the $FeNO^{2+}$ extinction coefficient, NO was bubbled through a 6×10^{-4} M Fe^{2+} solution in 1 M $HClO_4$ and a spectrum was taken. Maxima were observed at 450 and 580 nm with $\epsilon_{450} = 80$, $\epsilon_{580} = 25$. These values probably constitute lower limits, since the absorbance fades at a significant rate.

Potentiometric Analysis. Measurements were made using a Radiometer TT1 automatic titrator equipped with Radiometer P101 platinum redox electrode and a calomel reference electrode. No absolute calibration was made.

Acknowledgments. This work was supported in part by National Science Foundation Grant CHE 7905911, by an NIH Institutional Biomedical Sciences Support Grant, by a

Dreyfus Foundation Teacher-Scholar Award to I.R.E., and by NIH Research Grant GM 08893.

References and Notes

(1) Gossart, E. *C. R. Acad. Sci.* **1847**, *24*, 21.
(2) Swift, E. H. "A System of Chemical Analysis for the Common Elements"; W. H. Freeman: San Francisco, 1939; pp 485–486.
(3) Hac, R.; Netuka, V. *Collect. Czech. Chem. Commun.* **1929**, *1*, 521.
(4) Kolthoff, I. M.; Sandell, E. B.; Moskovitz, B. *J. Am. Chem. Soc.* **1933**, *55*, 1454.
(5) Savolainen, J. E. "On the Kinetics of Oxidation by Nitric Acid", ORNL CF 58-6-119; Oak Ridge National Laboratory: Oak Ridge, Tenn., 1958.
(6) Abel, E.; Schmid, H.; Poliak, F. *Monatsh. Chem.* **1936**, *69*, 125.
(7) Abel, E.; Schmid, H. *Z. Phys. Chem. (Leipzig)* **1928**, *132*, 56, 64; **1928**, *134*, 279; **1928**, *136*, 430.
(8) Abel, E.; Schmid, H.; Babad, S. *Z. Phys. Chem. (Leipzig)* **1928**, *136*, 135, 419.
(9) For reviews see: (a) Gray, P.; Yoffee, A. D. *Chem. Rev.* **1955**, *55*, 1069. (b) Turney, T. A.; Wright, G. A. *Ibid.* **1959**, *59*, 497. (c) "Recent Aspects of the Inorganic Chemistry of Nitrogen", *Chem. Soc., Spec. Publ.* **1957**, *No. 10.*
(10) Kustin, K.; Taub, I. A.; Weinstock, E. *Inorg. Chem.* **1966**, *5*, 1079.
(11) Latimer, W. M. "Oxidation Potentials", 2nd ed.; Prentice-Hall: Englewood Cliffs, N.J., 1952.
(12) Schmid, G.; Bähr, G. *Z. Phys. Chem. (Frankfurt am Main)* **1964**, *41*, 8.
(13) Denbigh, K. G.; Prince, A. J. *J. Chem. Soc.* **1947**, 790.
(14) Winkler, L. W. *Ber.* **1901**, *24*, 1409.
(15) Schmid, H.; Marchgraber, R.; Dunki, F. *Z. Elektrochem.* **1937**, *43*, 337.
(16) Bodenstein, M.; Boes, F. *Z. Phys. Chem. (Leipzig)* **1922**, *100*, 75.
(17) Abel, E.; Proisl, J. *Z. Elektrochem.* **1929**, *35*, 712.
(18) Manchot, W.; Hannschild, H. *Z. Anorg. Allg. Chem.* **1924**, *140*, 22.
(19) Matheson, M. S.; Dorfman, L. M. "Pulse Radiolysis"; M.I.T. Press: Cambridge, Mass., 1969; pp 110–111.
(20) Substitution on ferrous ion is known to be rapid (ref 10). However, nitrate does not readily form complexes, so that the equilibrium in reaction 22 should lie far to the left. A steady-state analysis of reactions 22–23 yields a complex rate law for step P1, which reduces to any of several forms, including eq 20–21 depending upon the relative values of the rate constants in eq 22–23. In view of the uncertainties in these parameters, we prefer to use the simpler rate equations (20)–(21) in our computer simulations. Trial calculations suggest that the precise form chosen for v_1 and v_{-1} does not markedly affect the reaction profile.
(21) Pathway (a) might also proceed via an NO_2^{2-} intermediate with a mechanism analogous to that of eq 18 and 19. See: Jolly, W. L. "Inorganic Chemistry of Nitrogen"; W. A. Benjamin: New York, 1964; p 77, for a discussion of NO_2^{2-}.
(22) Rabani, J.; Mulac, W. A.; Matheson, M. S. *J. Phys. Chem.* **1965**, *69*, 53.
(23) Bunton, C. A.; Llewellyn, D. R.; Stedman, G. in ref 9c, p 113.
(24) Holmesland, B. *Tidsskr. Kjemi Bergves.* **1926**, *6*, 107.
(25) Cotton, F. A.; Wilkinson, G. "Advanced Inorganic Chemistry", 3rd ed.; Interscience: New York, 1972; p 179.
(26) Hindmarsh, A. C. "Gear: Ordinary Differential Equation System Solver", Technical Report No. U010-3001, Rev. 2; Lawrence Livermore Laboratory: 1972.
(27) Gear, C. W. "Numerical Initial Value Problems in Ordinary Differential Equations"; Prentice-Hall: Englewood Cliffs, N.J., 1971; Chapter 11.
(28) Borok, M. T. *J. Appl. Chem. USSR (Engl. Transl.)* **1960**, *33*, 1742.
(29) Cysewski, G. R.; Prausnitz, J. M. *Ind. Eng. Chem. Fundam.* **1976**, *15*, 304.
(30) Harned, H. S.; Owen, B. B. "Physical Chemistry of Electrolytic Solutions"; Reinhold: New York, 1943; pp 34–37.
(31) "Symposium on Reaction Mechanisms, Models and Computers", *J. Phys. Chem.* **1977**, *81*, No. 25. Edelson, D. *J. Chem. Educ.* **1975**, *52*, 642.
(32) Edelson, D.; Field, R. J.; Noyes, R. M. *Int. J. Chem. Kinet.* **1975**, *7*, 417. Edelson, D.; Noyes, R. M.; Field, R. J. *Ibid.* **1979**, *11*, 155.
(33) Brummer, J. G.; Field, R. J. *J. Phys. Chem.* **1979**, *83*, 2328.
(34) Sullivan, J. C.; Thompson, R. C. *Inorg. Chem.* **1979**, *18*, 2375.
(35) Grätzel, M.; Henglein, A.; Lilie, J.; Beck, G. *Ber. Bunsenges. Phys. Chem.* **1969**, *73*, 646. $K15 = 6.54 \times 10^4\ M^{-1}$, $k_5 = 6.5 \times 10^7\ M^{-1}\ s^{-1}$. The rate constants reported for reaction 15 also support our assumption that this reaction may be taken to be at equilibrium.
(36) Grätzel, M.; Taniguchi, S.; Henglein, A. *Ber. Bunsenges. Phys. Chem.* **1970**, *74*, 488. $K16 = 7.3 \times 10^{-5}$ M, $k_{-6} = 7.3 \times 10^7\ M^{-1}\ s^{-1}$.
(37) Stedman, G. *Adv. Inorg. Chem. Radiochem.* **1979**, *22*, 113.
(38) Field, R. J.; Körös, E.; Noyes, R. M. *J. Am. Chem. Soc.* **1972**, *94*, 8649.

Oxidative Addition of Aryl Carboxylates to Ni(0) Complexes Involving Cleavage of the Acyl–O Bond

Takakazu Yamamoto,* Junichi Ishizu, Teiji Kohara, Sanshiro Komiya, and Akio Yamamoto*

Contribution from the Research Laboratory of Resources Utilization, Tokyo Institute of Technology, 4259 Nagatsuta, Midori-ku, Yokohama 227, Japan.
Received January 2, 1980

Abstract: Reactions of aryl carboxylates RCOO-*p*-C_6H_4X (R = CH_3, C_2H_5, *n*-C_3H_7; X = H, CH_3, OCH_3, CN) with bis(1,5-cyclooctadiene)nickel, $Ni(cod)_2$, in the presence of phosphine ligands yield olefin (R(-H)), *p*-XC_6H_4OH, and nickel carbonyl complex(es) when the R group has a β hydrogen, whereas CH_4, C_2H_6, nickel carbonyl complex(es), and nickel phenoxide are formed when the R group is CH_3. The formation of the products is accounted for by assuming oxidative addition of the ester to nickel involving the cleavage of the acyl–O bond of RCOO-*p*-C_6H_4X followed by decarbonylation of the acylnickel complex and decomposition of the alkylnickel complex: RCOO-*p*-$C_6H_4X + NiL_n \rightarrow RCONiL_nOC_6H_4X \rightarrow RNiL_nOC_6H_4X + CO$. The intermediate alkyl(phenoxo)nickel-type complex $NiCH_3(OC_6H_5)$(bpy) was in fact isolated in the reaction of phenyl acetate with $Ni(cod)_2$ in the presence of 2,2′-bipyridine. The rate of the reaction is first order with respect to the concentration of the zerovalent nickel complex and the pseudo-first-order rate constant increases with the increase in the basicity of the phosphine ligand added and with the increase in the electron-withdrawing ability of X. On the basis of these results a mechanism involving a nucleophilic attack at the carbonyl carbon by nickel is proposed. The activation parameters for the reaction of $C_2H_5COOC_6H_5$ with the mixture of $Ni(cod)_2$ and PPh_3 are $\Delta H^{\ddagger} = 21 \pm 2$ kcal/mol, $\Delta S^{\ddagger} = -8.8 \pm 2.9$ eu.

Introduction

Although cleavage of an ester bond catalyzed by an alkali and acid has been extensively studied, activation and cleavage of the ester bond by a transition-metal complex in nonaqueous solvents are the subject of recent interest.[1-7] Some of the transition metal promoted cleavage reactions of the allyl–O bonds of allyl esters have been utilized for organic synthesis[6] and preparation of π-allyl complexes.[1,7]

In spite of the increasing interest concerning the transition metal promoted C–O bond cleavage of esters a detailed study of the reaction process has not been made. Previously we reported in a communication form the following two types of oxidative additions of esters to Ni(0) complexes and that the mode of the scission of the ester bond depends on the ester employed and the ligand coordinated to nickel:[8]

$$RCOOR' + NiL_n \rightarrow RCONiL_nOR' \text{ (type A)} \quad (1)$$

$$RCOOR' + NiL_n \rightarrow RCOONiL_nR' \text{ (type B)} \quad (2)$$

0002-7863/80/1502-3758$01.00/0